International Journal of Nanomaterials, Nanotechnology and Nanomedicine

Mohammad A Wahab[1]*, Farzana Darain[1#], Azharul Karim[2] and Jorge N Beltramini[1]

[1]NANOMAC (ARC Nanomaterials Centre) AIBN, UQ, [1#]Australian Institute of Bioengineering and Nanotechnology (AIBN), The University of Queensland, St Lucia, Brisbane, QLD 4072, Queensland, Australia

[2]Chemistry, Physics and Mechanical Engineering, Science and Engineering Faculty, Queensland University of Technology, 2 George Street, QLD 4001 Australia

Dates: Received: 25 May, 2015; **Accepted:** 31 July, 2015; **Published:** 05 August, 2015

***Corresponding author:** Mohammad A Wahab, NANOMAC (ARC Nanomaterials Centre) AIBN, UQ, Australian Institute of Bioengineering and Nanotechnology (AIBN), The University of Queensland, St Lucia, Brisbane, QLD 4072, Queensland, Australia, Tel: +6133463817; Fax: +61 7 3346 397; E-mail: m.wahab@uq.edu.au

www.peertechz.com

ISSN: 2455-3492

Keywords: Fullerene mesoporous carbon; Nano-hard template; Protein immobilization; Carbon; Bovine serum albumin

Short Communication

Nano-Confined Synthesis of Fullerene Mesoporous Carbon (C_{60}-FMC) with Bimodal Pores: XRD, TEM, Structural Properties, NMR, and Protein Immobilization

Abstract

Nanoconfined synthesized crystalline fullerene mesoporous carbon (C_{60}-FMC) with bimodal pore architectures of 4.95 nm and 10-15 nm pore sizes characterized by XRD, TEM, nitrogen adsorption/desorption isotherm and solid-state NMR, and the material was used for protein immobilization. The solid-state ^{13}C NMR spectrum of C_{60}-FMC along with XRD, BET and TEM confirms the formation of fullerene mesoporous carbon structure C_{60}-FMC. The immobilization of albumin (from bovine serum, BSA) protein biomolecule in a buffer solution at pH 4.7 was used to determine the adsorption properties of the C_{60}-FMC material and its structural changes investigated by FT-IR. We demonstrated that the C_{60}-FMC with high surface area and pore volumes have excellent adsorption capacity towards BSA protein molecule. Protein adsorption experiments clearly showed that the C_{60}-FMC with bimodal pore architectures (4.95 nm and 10-15 nm) are suitable material to be used for protein adsorption.

Introduction

The immobilization of biomolecules onto porous solid supports has attracted much attention due to its scientific, technological importance and application in many areas, such as bio catalysis, separation and transport, immobilization, advanced materials (electrode materials), adsorption science, and nanobiotechnology [1-9]. Meanwhile, different porous solid materials (silica, inorganic oxides, carbon etc.) have been considered as support for the adsorption of biomolecules [1-3]. For example, much progress on the adsorption of biomolecules onto nanoporous silica materials has been reported but the use of porous silica supports usually deteriorate the native characteristics of a protein molecule and even leads to the loss of its coherent structure due to the electrostatic interactions between the –OH groups of silica and the surface charge on the amino acid residues on the surface of the proteins [1-10]. It was also reported that the structure of the porous silica adsorbent in aqueous media is not stable due to the hydrolysis of their siloxane bridges (≡Si-O-Si≡) although the efficiency of biochemical devices largely depends on the stability of solid supports/adsorbents and solid support-protein interactions [1-8,11]. Therefore, new porous adsorbents structures need to be found that can be effectively used in the development of nanobiomedical devices. In this context, recently thermo-mechanically robust porous carbon materials that are very suitable for bio-applications have received much attention due to their unique characteristics, namely: a large specific surface area and high pore volume with pore sizes distribution that can be tuned over a wide pore range of 2 nm to > 50 nm [12]. At the same time, several examples of enzyme immobilization and biomolecules or drugs adsorption on mesoporous carbons have been reported in the literatures [13-20]. It is also observed that mesoporous carbon materials exhibited better performance for these applications than that of counterpart silica material. Then, instead of using a conventional carbon source as mentioned above [1-4,12-20] it will be necessary to find a new carbon source to create a new mesoporous carbon solid framework that will improve the adsorption of biomolecules. As such, Fullerenes (C_{60}) as carbon source consists of nanoscopic building block with surface tailorable that can give unique functionalities to the mesoporous carbon framework [21-23]. Previously, fullerene C_{60} has been partly used along with porous silica for extending their surface functionalities [24-32] but C_{60} has not been reported to be used as sole carbon source for preparing fullerene mesoporous carbon that can be useful for protein immobilization.

With this concept in mind, this paper, successfully demonstrate the use of fullerene C_{60} as carbon source to prepare a new class of fullerene mesoporous carbon (C_{60}-FMC) with bimodal pore architectures via pore filling method and its properties for protein immobilization.

Experimental Section

Materials

Tetraethylorthosilicate (TEOS), Pluronic surfactant P123 (EO20PPO70EO20), Fullerene C_{60}, Trimethylbenzene (TMB) and Albumin from Bovine serum (BSA) from Sigma-Aldrich were used as received without further purification.

Synthesis of mesoporous SBA-15 silica nano-hard template

In order to prepare mesoporous SBA-15 template, first 2 g of Pluronic surfactant P123 ($EO_{20}PPO_{70}EO_{20}$) was stirred in 60 ml of 2M HCl at 38 °C for 2 h for making a homogenous solution. Then 4.2 g of TEOS precursor was added to the above surfactant containing acidic solution. The mixture was stirred for only 6-8 min and then left the solution to stand for 24 h at 38 °C [29,30]. The mixture was subsequently transferred into an autoclave for another 24 h at 100 °C. The as-synthesized SBA-15 silica was collected by filtration, dried and then calcined at 550 °C for 6 h in air to remove surfactant.

Nano-confined synthesis of fullerene mesoporous carbon (C60-FMC)

A pore fill nanocasting method was used for the synthesis of high surface area fullerene mesoporous carbon (C_{60}-FMC) by using mesoporous SBA15 silica as a hard template [12,30]. A targeted amount of fullerene C_{60} was added into trimethylbenzene in the appropriate proportion and then sonicated for few hours. Afterwards, the sonicated solution was thoroughly mixed with mesoporous SBA-15 silica template. Then the fullerene impregnated SBA-15 composite was heated at 100 °C for 6 h and later temperature was increased to 160 °C holding for another 6 h for polymerization. Then the polymerized fullerene C_{60}/silica nanocomposite material was transferred into an aluminum quartz boat that was placed at the middle of a tube furnace and carbonized at 850 °C under nitrogen atmosphere for 6 h. After heat-treatment, the mesoporous fullerene/silica nanocomposite was washed thoroughly with 5 wt% HF to remove silica template. As a result of this step a highly porous fullerene mesoporous carbon was created. Mesoporous SBA-15 silica template-free C_{60}-FMC samples were used for all subsequent characterization and application.

Adsorption study of BSA to fullerene mesoporous carbon (C60-FMC)

Prior to the adsorption studies, the fullerene mesoporous carbon materials were dried overnight at 120 °C. Then BSA was dissolved in 10 mM acetate buffer, pH 4.7 to prepare stock solution. 10 mg of the support samples were suspended in BSA solution and mixture was continuously shaken at 500 rpm at room temperature. The adsorption kinetics of BSA was recorded at various pre-determined time periods. Suspensions were separated by centrifugation at 10000 g for 3 min at room temperature and then 20 µL of supernatant were taken out for measurement of the protein concentration using NanoDrop® ND-1000 spectrophotometer at 280 nm. The amount of immobilized BSA protein was calculated by subtracting the amount of BSA in the supernatant liquid after adsorption from the amount of protein present before adding the samples. Finally, the BSA-immobilized C_{60}-FMC supports were washed three times with acetate buffer solution then separated by centrifugation and characterized using attenuated total reflection IR. A leaching test was carried out using BSA immobilized mesoporous materials suspended in 10 mM acetate buffer, pH 4.7 which was continuously shaken at 500 rpm at room temperature for 24 h. After centrifuging at 10000 g for 3 min, the amount of protein leakage was investigated using NanoDrop® ND-1000 spectrophotometer at 280 nm. The isoelectric point for BSA is at pH 4.7. Therefore, the protein stock solution for BSA was prepared in acetate buffer solution with a pH equal to its isoelecric point since proteins tended to bind well at or around their isoelectric point. In addition, at the isoelectric point, protein involved in hydrophobic interactions with the three-dimensional mesopore structure.

Characterization techniques

Mesoporous SBA15 silica nano-hard template and fullerene mesoporous carbon (C_{60}-FMC) materials were comprehensively characterized by using X-ray diffraction (XRD, Bruker D8 Advanced X-ray diffractometer with Ni-filtered CuKa radiation at a voltage of 40 mV and a current of 30 mA) to confirm the formation of fullerene mesoporous carbon (C_{60}-FMC) structure, whereas transmission electron microscope (TEM) was used to determine the pore structure of C_{60}-FMC. TEM (TEM, FEI Tecnai 20, 200kV) imaging was carried out on a F20 microscope with an accelerating voltage 200 kV. The dispersed particles in ethanol were undergone for Ultra sonication for 10 min for ensuring good dispersion and homogeneity of particles in ethanol. The solution was then settled on carbon coated Cu grids for TEM imaging. X-ray diffraction (XRD) patterns were also recorded on a Rigaku Miniflex diffractometer (Japan) with Cu Kα radiation (λ=0.154 nm) at a scanning rate of 2 degree/min in the 2θ range from 10 to 80°. The BET surface areas and textural properties were obtained using an automated adsorption analyzer (Quadrasorb SI, Quantachrome, USA). The N2-adsorption–desorption isotherms were measured at 77 K on a nitrogen-adsorption apparatus after degassing the samples at 180 °C for 6 h. The Brunauer–Emmett–Teller (BET) surface areas were determined at a relative pressure (P/Po) of 0.3005. The pore-size distribution (PSD) was obtained by using the Barrett-Joyner-Halenda (BJH) model from the desorption branch (31,32). Then the attenuated total reflection FT-IR spectra of BSA-immobilized mesoporous supports were obtained using a Thermo Nicolet 5700 spectrometer. The measurement was based on 32 scans with a resolution of 4 cm^{-1}. The samples were scanned in the spectral range of 1800–1200 cm^{-1}. Solid-state NMR was performed on the Avance III spectrometer (Bruker), operating at 75.468 MHz for ^{13}C. The samples were placed in the 4 mm zirconium rotor and rotated at magic angle with 5 kHz frequency. The spectra were recorded using SP-hpdec technique (single pulse with high power proton decoupling). The parameters included 42ms acquisition time with sweep width of 50 kHz; 2K data points were collected. High-power decoupling utilized tppm15 scheme at 65.7 kHz proton power. Between 200 and 7000 scans were collected. The recycle times were from 10s to 60s, according to the sample's T1.

Results and Discussion

Preparation and structural features of mesoporous SBA15 nano-hard template

In order to prepare fullerene mesoporous carbon, meosoporous SBA-15 silica template needs to show a very ordered structure with large pore size that allows the impregnation of fullerene C_{60} inside the

Citation: Wahab MA, Darain F, Karim A, Beltramini JN (2016) Nano-Confined Synthesis of Fullerene Mesoporous Carbon (C_{60}-FMC) with Bimodal Pores: XRD, TEM, Structural Properties, NMR, and Protein Immobilization. Int J Nanomater Nanotechnol Nanomed 2(1): 001-008. DOI: 10.17352/2455-3492.000006

SBA-15 silica pores. As shown in Figure 1, the silica based SBA-15 has three well-resolved peaks at 2° values between 0.75 and 5°, indicating the formation of hexagonal mesoporous SBA15 silica material, which is also supported by the TEM images in Figure 2. The fact that the type IV N_2 adsorption-desorption isotherms confirm the mesoporous structure of the SBA-15 silica with capillary condensation step at relative pressure of 0.618 to 0.81, corresponding to the existence of mesopores with narrow pore size distribution as shown in Figure 3 (inset) [11,33-36]. The specific surface area (SBET), total pore volume, and BJH pore size of the highly ordered mesoporous SBA15 silicate were 719 m^2/g, 1.12 cm^3/g and 9.15 nm, respectively. The textural properties are in good consistency with previous results on the highly ordered mesoporous SBA-15 silicate.

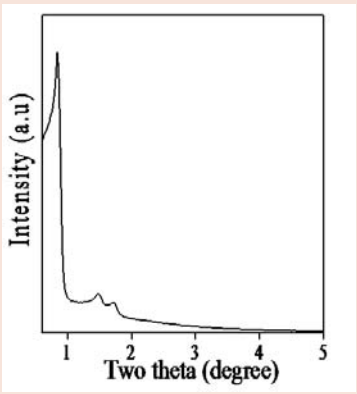

Figure 1: Small angle XRD pattern of mesoporous SBA15 silicate..

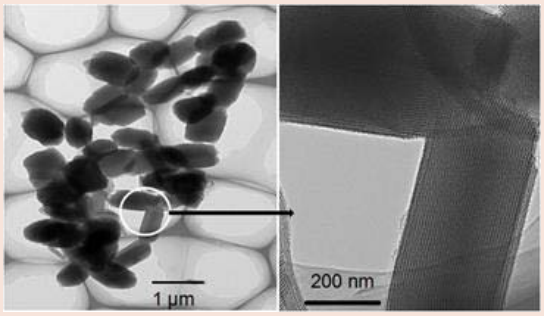

Figure 2: TEM image of mesoporous SBA15 silicate: (a) low magnification and (b) high magnification.

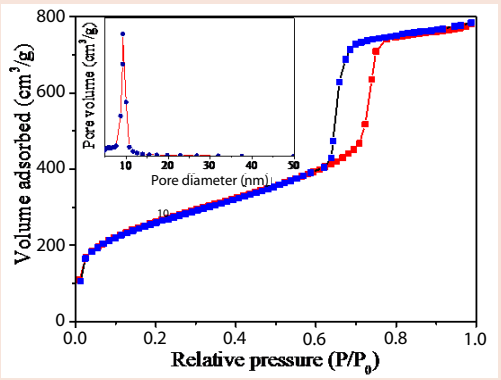

Figure 3: N2 adsorption–desorption isotherms and pore size distribution (inset) of calcined mesoporous SBA15 silica.

Nano-confined synthesis and properties of fullerene mesoporous carbon (C_{60}-FMC) from Fullerene C_{60} carbon source and meosporous SBA15 as nano-hard template

As discussed before well-ordered fullerene mesoporous carbon were prepared by homogenous pore filling of the mesoporous SBA15 silica template with the fullerene carbon source solution. Figure 4 schematically shows the preparation steps of the fullerene mesoporous carbon (C_{60}-FMC) materials. Small and high angle XRD measurements were carried out on fullerene mesoporous carbon after removal of SBA-15 silica template. XRD patterns of the resultant C_{60}-FMC are shown in Figure 5. It can easily be seen that synthesized C_{60}-FMC appears to be well-ordered showing periodicity in the mesoscale range as evidenced by the sharp and intense peaks in the region around 0.96 2θ and another broad peak at about 1.60-1.65 2θ. This finding is consisting with the case of a well-ordered mesoporous material with uniform framework mesopores distribution [12,16-19,34-39]. Small angle XRD for pure Fullerene C_{60} carbon source sample was also carried out and no peak was observed suggesting that the fullerene mesoporous carbon framework was formed as a result of the nano-hard templating step. The C_{60}-FMC shows few peaks in the high angle XRD pattern (Figure 5b), indicating the presence of graphitic carbon in fullerene mesoporous carbon framework.

To confirm the mesoporous structure, the C_{60}-FMC sample was analyzed by TEM. The highly organized pore channels are results when hard-templating impregnation method that can be seen in Figure 6. In addition, TEM inset image in Figure 6 shows the presence of disordered interconnected large mesopores in the C_{60}-FMC sample. By combining the XRD pattern and the TEM observation, it could be concluded that C_{60}-FMC is stable after removal of silica template. N_2 adsorption-desorption experiments shows that the specific surface area (S_{BET}), total pore volume, and BJH pore size of the fullerene mesoporous carbon materials were 643 m^2/g, 0.67 cm^3/g and 4.95 nm, respectively [15-17]. As shown in Figure 7a, N_2 sorption isotherm of C_{60}-FMC displays different adsorption-desorption behavior with the presence of two hysteresis loops that indicate the presence of two different pore systems in one material. Figure 7a shows type-IV curves with a sharp capillary condensation step in the relative pressure range of 0.45–0.75 and a H1-type hysteresis loop, indicative of uniform cylindrical organized mesopores in the final framework [34-39].

In addition there is one more hysteresis loop at higher pressure range of 0.82 to 1. As shown in Figure 7b, the maxima of the pore size distributions calculated from desorption step by the BJH method are 4.95 nm and 12.5 nm respectively. The secondary mesopore framework is in the broad range of 10-15 nm. This behavior could be resulting

Citation: Wahab MA, Darain F, Karim A, Beltramini JN (2016) Nano-Confined Synthesis of Fullerene Mesoporous Carbon (C_{60}-FMC) with Bimodal Pores: XRD, TEM, Structural Properties, NMR, and Protein Immobilization. Int J Nanomater Nanotechnol Nanomed 2(1): 001-008. DOI: 10.17352/2455-3492.000006

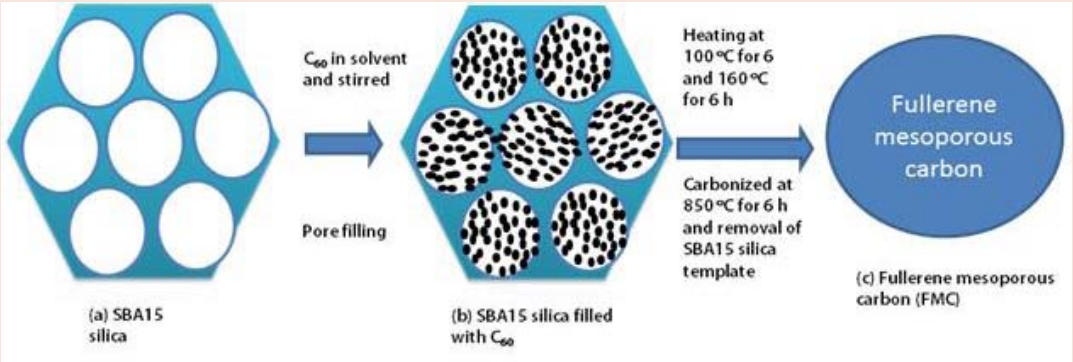

Figure 4: Synthesis of fullerene mesoporous carbon from hard template mesoporous SBA15 silicate.

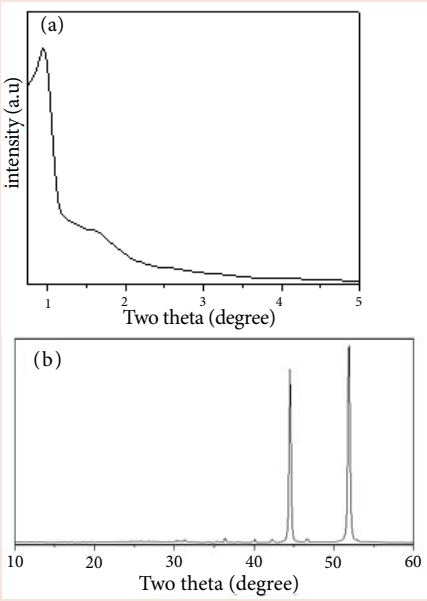

Figure 5: Fullerene mesoporous carbon (a) small angle XRD and (b) higher angle XRD patterns.

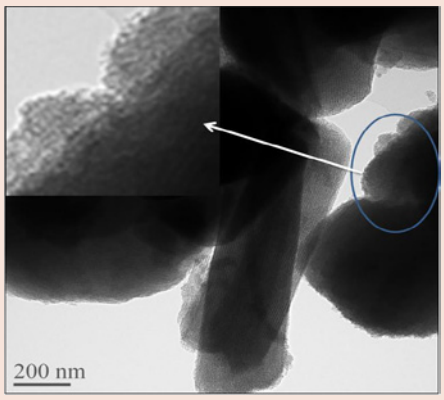

Figure 6: TEM image of fullerene mesoporous carbon and inset show the circular area for clear visualization.

from the carbon source loading that blocks some nanopores of the SBA-15 silica template. However, according to the isotherm shape of C_{60}-FMC (Figure 7a), a pore restriction caused by in-bottle pores, seems to be the more likely explanation. The narrower pore mouths may be caused by enhanced carbon deposition at the entrance and/or by more narrow voids between blocked adjacent tube channels. This could be the results of presence of large mesopores and/or also the formation of some disordered like-pores in the framework [40,41]. These results clearly demonstrate the possibility of synthesizing uniform FMC with bimodal pore architectures.

NMR characterization

The solid-state ^{13}C NMR spectroscopy spectra of pure C_{60} and C_{60}-FMC (fullerene mesoporous carbon after removing silica from carbonized silica/fullerene composite at 850 ^{O}C) are shown in Figure 8. The spectrum of pure C_{60} in Figure 8a shows sharp signal at 143 ppm that corresponds to the C_{60} itself. The result is consistent with previously reported NMR spectrum of pure fullerene C_{60}. For the fullerene mesoporous carbon after removing silica template, the ^{13}C NMR spectrum of C_{60}-FMC becomes broad and shifted to the right side as shown in Figure 8b. The large width peak may be due to (i) confinement of the C_{60} molecule inside nanopores of SBA15 template and removal of SBA15 template by HF washing for creating C_{60}-FMC via present nano-template synthesis procedure. Recently similar broad peak for synthesis of a periodic mesoporous organosilica (PMO) that contains a multiply bonded C_{60} moiety integrated into the silica channel walls of the mesoporous material and our results are consistent with previous NMR data in which fullerene C_{60} was confined into nanochannel of MCM-51 or MCM-48 via post-addition methods [23-28].

The adsorption performance of fullerene mesoporous carbon materials and leaching out experiment

The adsorption performance of fullerene mesoporous carbon materials as support materials for protein immobilization was carried out using a buffer solution at pH 4.7 at room temperature on a NanoDrop® ND-1000 spectrophotometer at 280 nm. Previously it has been reported that adsorption behavior of biomolecules depends

Citation: Wahab MA, Darain F, Karim A, Beltramini JN (2016) Nano-Confined Synthesis of Fullerene Mesoporous Carbon (C_{60}-FMC) with Bimodal Pores: XRD, TEM, Structural Properties, NMR, and Protein Immobilization. Int J Nanomater Nanotechnol Nanomed 2(1): 001-008. DOI: 10.17352/2455-3492.000006

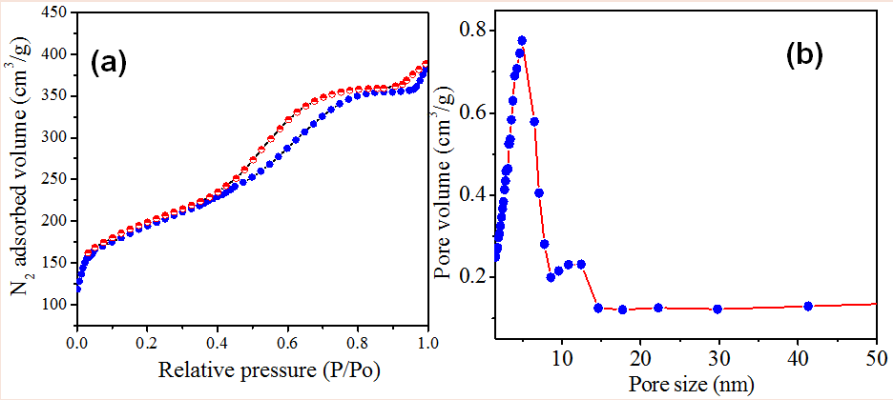

Figure 7: Fullerene mesoporous carbon : (a) nitrogen adsorption –desorption isotherms and (b) pore size distribution.

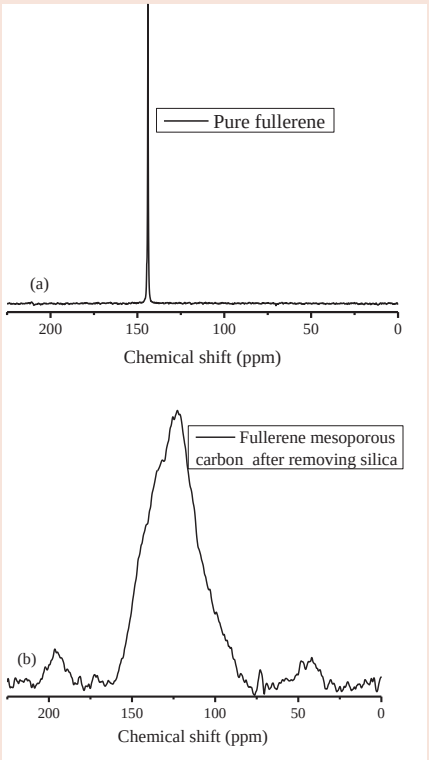

Figure 8: Solid-state 13C NMR spectroscopy spectra of (a) pure C60 and (b) C60-FMC (fullerene mesoporous carbon after removing silica from carbonized silica/fullerene composite at 850OC).

on the type of protein molecules and nature of solid supports [1-16,13-20,48-52]. In our case dimensions of BSA are 4.7 nm × 4.7 nm × 11 nm, whereas C_{60}-FMC adsorbent shows characteristics of bimodal pore size of 4.95 nm and 10-15 nm. The results in Figure 9 compare the adsorption of BSA on pure fullerene (F) and fullerene mesoporous carbon (C_{60}-FMC). Highly porous C_{60}-FMC with surface area 643 m^2/g bimodal pore sizes (4.95 nm and large pore about 10-15 nm), and pore volume 0.57 cm^3/g showed excellent adsorption capacity towards BSA protein molecules than that of pure non-porous fullerene. The differences in results as seen in Figure 9 could be attributed to the functional textural properties of C_{60}-FMC. For example, when adsorption time reaches 3 h, C_{60}-FMC sample shows about 70% adsorption capacity compared with only 24% adsorption capacity on pure non-porous fullerene structure. This remarkable adsorption capacity of C_{60}-FMC increases to 92% for C_{60}-FMC vs 35% for pure Fullerene when time reaches 20 h, clearly indicating that the textural properties such as pore architectures, high surface area and pore volume in C_{60}-FMC play an important role for the adsorption of BSA molecules [10,19,47,48]. An important consideration is to investigate whether the immobilized protein is leaching from the C_{60}-FMC support. The leaching tests were carried out with the BSA-immobilized C_{60}-FMC suspended in 10 mM acetate buffer at pH 4.7 which was continuously shaken at 500 rpm at room temperature for 24 h. It was confirmed that there is no or negligible leaching of protein from the C_{60}-FMC support to the buffered medium. Furthermore, the relative small pore size (4.95 nm) of C_{60}-FMC easily allows accommodating smaller size (4.7 nm) of BSA molecules inside pores of C_{60}-FMC under tested conditions. In addition, C_{60}-FMC shows large interconnected mesopores (10-15 nm) which allow in adsorbing more BSA in the framework of C_{60}-FMC.

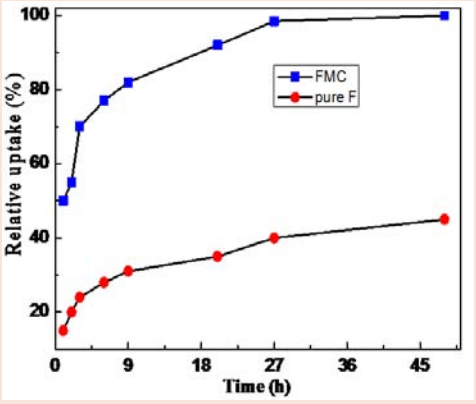

Figure 9: Adsorption kinetics of Bovine serum albumin (BSA) on fullerene mesoporous carbon C60-FMC and pure fullerene (F).

Citation: Wahab MA, Darain F, Karim A, Beltramini JN (2016) Nano-Confined Synthesis of Fullerene Mesoporous Carbon (C_{60}-FMC) with Bimodal Pores: XRD, TEM, Structural Properties, NMR, and Protein Immobilization. Int J Nanomater Nanotechnol Nanomed 2(1): 001-008. DOI: 10.17352/2455-3492.000006

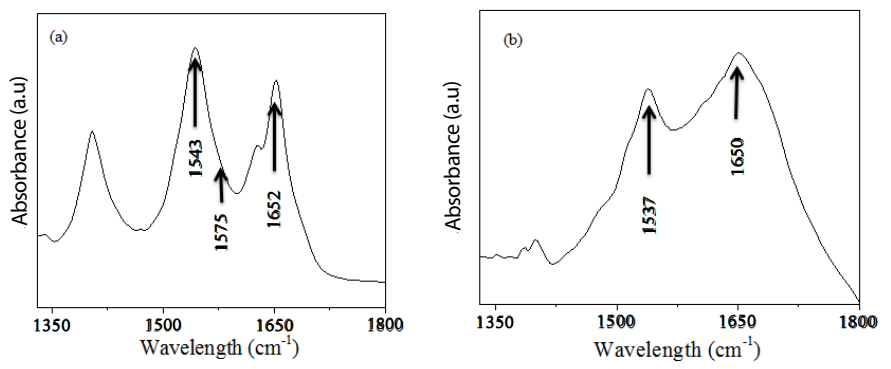

Figure 10: FT-IR spectra of (a) Bovine serum albumin (BSA) and (b) C60-FMC loaded with BSA.

FT-IR spectra of pure BSA and C_{60}-FMC-loaded with BSA

FT-IR spectra were widely used to investigate the structural stability of protein loaded on porous host in comparison to pure protein by observing their structural bands (amide I and amide II) after adsorption. In this study, IR spectra of pure BSA and C_{60}-FMC loaded with BSA are shown in Figure 10 at room temperature. The pure BSA sample in Figure 10a clearly shows the amide band I at near 1652 cm^{-1} (C=O stretching mode) and the amide band II at near 1543 cm^{-1}, (stretching mode of N-H) whereas the disappearance of the amide II N-H stretching mode is used to consider for unfolding of the protein (10,43-46). Figure 10b shows the IR spectrum of C_{60}-FMC loaded with BSA. The presence of two major bands centered at 1649 and 1537 cm^{-1} for C_{60}-FMC loaded BSA sample indicates successful adsorption of BSA onto C_{60}-FMC [10,43-47]. In this study, IR adsorption bands of pure BSA as stated in Figure 8a become broadened when BSA is loaded into C_{60}-FMC sample. This behavior could be interpreted by the fact that adsorption of BSA on the C_{60}-FMC adsorbent might be accompanied by the partial transformation of the CONH peptide group arrangement from typical α-helices to β-sheets, which could also be indicative of the broadened frequency parts of the absorption bands in the amide I and amide II ranges. The change in the peptide group arrangement can also be seen from the change in the relative intensities of the absorption bands at 1652 cm^{-1} and 1547 cm^{-1}. Similar IR spectra of porous materials loaded biomolecules have been previously reported [10,43-44].

Conclusions

Novel fullerene mesoporous carbon molecular sieves (C_{60}-FMC) with bimodal pore distribution consisting of mesopores in the range of 4.95 nm and 10-15 nm where mesoporous SBA-15 silica was used nano-hard template. The solid-state ^{13}C NMR spectrum of C_{60}-FMC along with XRD, BET and TEM clearly confirms the formation of fullerene mesoporous carbon structure C_{60}-FMC. The C_{60}-FMC showed excellent properties for protein immobilization. The adsorption of BSA protein on C_{60}-FMC carbon showed that the textural properties of the adsorbent affect the shape of the relative uptake and the maximum adsorption of the protein. For example, C_{60}-FMC has provided excellent adsorption capacity than pure non-porous fullerene. It has been found that the amount of BSA adsorption was related to the pore volume, surface area and pore size of C_{60}-FMC. The presence of amide band I and the amide band II of BSA protein molecule, due to the C=O stretching mode, and stretching mode of N-H vibrations respectively has been confirmed by FT-IR spectroscopy. This study also suggested that CONH peptide group arrangement of the protein typical of α-helices partially transforms into that of β-sheets when BSA is adsorbed by porous C_{60}-FMC. Thus, the outcomes from this study on the immobilization of BSA on C_{60}-FMC adsorbent nanocarriers with different textural properties and nature of the surface of carriers enable to differentiate adsorption behaviors of the protein–adsorbent system. In summary, this protein immobilization on fullerene mesoporous carbon host allows researchers to exploit the tunable properties of proteins to design protein-based Nano devices.

Acknowledgement

Authors thank the ARC Centre and AIBN-UQ providing the grant and research fund and facilities at ARC Centre for Functional Nano materials, AIBN UQ. We acknowledge the facilities and the scientific and technical assistance of the Australian Microscopy and Microanalysis Research Facility at the Centre for Microscopy and Microanalysis, University of Queensland, Brisbane, Australia.

References

1. Vallet MV, Balas F, Arcos D (2007) Mesoporous materials for drug delivery. Angew Chem Int Edn 46: 7548-7558.
2. Qin GW, Darain F, Wang H, Dimitrov K (2011) Surface modification of permalloy ($Ni_{80}Fe_{20}$) nanoparticles for biomedical applications. J Nanopart Res 13: 45-51.
3. Mayoral A, Arenal R, Gascn V, Mrquezlvarez C, Blanco RM, et al. (2013) Designing functionalized mesoporous materials for enzyme immobilization: locating enzymes by using advanced TEM techniques. Chem Cat Chem 5: 903-909.
4. Wahab MA, He CB (2011) Hydrothermally stable periodic mesoporous ethane-silica and bimodal mesoporous nanostructures.. J Nanosci Nanotechnol 11: 8481-8487.
5. Vandenberg ET, Brown RS, Krull UJ (1983) In immobilized Biosystems in

Citation: Wahab MA, Darain F, Karim A, Beltramini JN (2016) Nano-Confined Synthesis of Fullerene Mesoporous Carbon (C_{60}-FMC) with Bimodal Pores: XRD, TEM, Structural Properties, NMR, and Protein Immobilization. Int J Nanomater Nanotechnol Nanomed 2(1): 001-008. DOI: 10.17352/2455-3492.000006

Theory and Practical Applications Elsevier, Holland, pp. 129–130.

6. Weetall HH (1993) Preparation of immobilized proteins covalently coupled through silane coupling agents to inorganic supports. App Biochem Biotech 41: 157-188.

7. Weetall HH (1988) In Analytical Use of Immobilized Biological Compounds for Detection, Medical and Industrial Uses, ed. By G.G. Guilbault, M. Mascini, D. Reidel Publishing Co, Boston, MA, pp. 1–2.

8. Wang Y, Caruso F (2005) Mesoporous silica spheres as supports for enzyme immobilization and encapsulation. Chem Mater 17: 953-961.

9. Fan J, Lei J, Wang L, Yu C, Tu B, et al. (2003) Rapid and high-capacity immobilization of enzymes based on mesoporous silicas with controlled morphologies. Chem Commun 2140-2141.

10. Park M., Park SS, Selvaraj M, Kim I, Zhao DY, et al. (2009) Hydrophobic mesoporous materials for immobilization of enzymes. Micropor Mesopor Mater 124: 76-83.

11. Zhao D, Feng J, Huo Q, Melosh N, Fredrickson GH, et al. (1998) Triblock copolymer syntheses of mesoporous silica with periodic 50 to 300 angstrom pores. Science 179: 548-552.

12. Jun S, Joo SH, Ryoo R, Kruk M, Jaroniec M, et al. (2000) Synthesis of new, nanoporous carbon with hexagonally ordered mesostructure. J Am Chem Soc 122: 10712-10713.

13. Moulton SE, Minett AI, Murphy R, Ryan KP, McCarthy D, et al. (2005) Biomolecules as selective dispersants for carbon nanotubes. Carbon 43: 1879-1884.

14. Vashist SK, Zheng D, Pastorin G, Al-Rubeaane K, Luong JHT, et al. (2011) Delivery of drugs and biomolecules using carbon nanotubes. Carbon 49: 4077-4097.

15. Xu DP, Yoon SH, Mochida I, Qiao WM, Wang YG, et al. (2008) Synthesis of mesoporous carbon and its adsorption property to biomolecules. Micropor Mesopor Mater 115: 461-468.

16. Lee D, Lee J, Kim J, Kim J, Na HB, et al. (2005) Simple fabrication of a highly sensitive and fast glucose biosensor using enzymes immobilized in mesocellular carbon foam. Adv Mater 17: 2828-2833.

17. Malik DJ, Warwick GL, Venturi M, Streat M, Hellgardt K (2004) Preparation of novel mesoporous carbons for the adsorption of an inflammatory cytokine (IL-1β). Biomaterials 25: 2933-2940.

18. Wahab MA, He CB (2009) Hydrogen-bond directed self-organized benzene-bridged nanostructured free-standing monolithic structures and films. Soft Mater 7: 79-92.

19. Zhu Y, Shen W, Dong X, Shi J (2005) Immobilization of hemoglobin on stable mesoporous multilamellar silica vesicles and their activity and stability. J Mater Res 20: 2682.

20. Wang Z, Liu X, Lv M, Meng J (2010) Simple synthesis of magnetic mesoporous FeNi/carbon composites with a large capacity for the immobilization of biomolecules. Carbon 48: 3182-3189.

21. Kroto HW, Heath JR, O'Brien SC, Curl RF (1985) C_{60}: buckminsterfullerene. Nature 318: 162.

22. Chupa JA, Xu S, Fobert FF, Robert MS, McCauley J PJr, et al. (1993) A monolayer of C_{60} tethered to the surface of an inorganic substrate: assembly and structure. J Am Chem Soc 115: 4383.

23. Hawkins JM (1992) Osmylation of C_{60}: Proof and characterization of the soccer-ball framework. Acc. Chem Res 25: 150-156.

24. Gu G, Ding W, Du Y, Huang H, Yang S (1997) C_{60} induced photoluminescence of a silica molecular sieve. Appl Phys Lett 70: 2619.

25. Garcia J, Bourdelande JL, Herance JR, Peris E, Vidal J, et al. (2005) Second harmonic generation of C_{60} incorporated in alkali metal ion zeolites and mesoporous. MCM-41 silica. Chem Mater 17: 4097-4102.

26. Govindaraj A, Nath M, Eswaramoorthy M (2000) Studies of C_{60} and C_{70} incorporated in cubic mesoporous silica (MCM-48). Chem Phys Lett 317: 35-39.

27. Mou CY, Lee CH, Lin TS, Lin HP, Zhao QS, et al. (2003) High loading of C_{60} in nanochannels of mesoporous MCM-41 materials. Micropor Mesopor Mater 57: 199-209.

28. Whitnall W, Cademartiri L, Ozin GA (2007) C_{60}−PMO: periodic mesoporous buckyballsilica. J Am Chem Soc 129: 15644-15649.

29. Shi-Zhao K, Die-er Y, Xiangqing L, Jin M (2013) Preparation and surface enhanced Raman scattering behavior of Ag-coated C60 nanoclusters. Appl Surf Sci, 286: 275-279.

30. Itzel J. Ramírez C, Victor ML, Taras Y, Gromovoyc M, et al. (2015) Solvent-free functionalization of fullerene C60 and pristine multi-walled carbon nanotubes with aromatic amines. Appl Surf Sci, 328: 45-62.

31. Maria B, Edgar AZ, Vladimir AB (2013) Adsorption of meso-tetraphenylporphines on thin films of C60 fullerene. Appl Surf Sci 275: 374-383.

32. Jiaguo Y, Tingting M, Gang L, Bei C (2011) Enhanced photocatalytic activity of bimodal mesoporous titania powders by C60 modification. Dalton Trans 2011, 40, 6635-6644.

33. Yu C, Fan J, Tian B, Zhao DY (2004) Morphology development of mesoporous materials: a colloidal phase separation mechanism. Chem Mater 16: 889-898.

34. Ji X, Kyu TL, Nazer LF (2009) A highly ordered nanostructured carbon–sulphur cathode for lithiumsulphur batteries. Nat Mater 8: 500506.

35. Brunauer S, Emmett PH, Teller E (1938) Adsorption of Gases in Multimolecular Layers. J Am Chem Soc 60: 309-319.

36. Barrett EP, Joyner LG, Halenda PP (1951) The Determination of pore volume and area distributions in porous substances. I. computations from nitrogen isotherms. J Am Chem Soc 73: 373-380.

37. Wahab MA, Jia Y, Yang DY, Zhao H, Yao XD (2013) Enhanced hydrogen desorption from Mg(BH4)2 by combining nanoconfinement and a Ni catalyst. J Mater Chem A 1: 3471-3478.

38. Wahab MA, Sudhakar S, Yeo E, Sellinger A (2008) Evaporation induced selfassembly of mesoscopically ordered organic/organosilica nanocomposite thin films with photoluminescent properties and improved hardness. Chem Mater 20: 1855-1861.

39. Mane GP, Dhawale DS, Anand C, Ariga K, Ji Q, et al. (2013) Selective sensing performance of mesoporous carbon nitride with a highly ordered porous structure prepared from 3-amino-1,2,4-triazine. J Mater Chem A 1: 2913-2920.

40. Katiyar A, Li L, Smirniotis PG, Pinto NG (2005) Adsorption of bovineserum albumin and lysozyme on siliceous MCM-41. Micropor Mesopor Matet 80: 311-320.

41. Wahab MA, Imae I, Kawakami Y, Ha CS (2005) Periodic mesoporous organosilica materials incorporating various organic functional groups: synthesis, structural characterization, and morphology. Chem Mater 17: 2165-2174.

42. Wahab MA, Ha CS (2005) Ruthenium-functionalised hybrid periodic mesoporous organosilicas: synthesis and structural characterization. J Mater Chem 15: 508-516.

43. Wahab MA, Kim I, Ha CS (2004) Hybrid periodic mesoporous organosilica materials prepared from 1,2-bis(triethoxysilyl)ethane and (3-cyanopropyl) triethoxysilane. Micropor Mesopor Mater 69: 19-27.

44. Chirgadze YN (1995) In Infrared Spectra and Structure of Polypeptides and Proteins, Moscow: Nauka.

45. Bellamy LJ (1975) In The Infrared Spectra of Complex Molecules, New York: Wiley.

46. Suzi G (1973) In Structure and Stability of Biological Macromolecules, Moscow.

Citation: *Wahab MA, Darain F, Karim A, Beltramini JN (2016) Nano-Confined Synthesis of Fullerene Mesoporous Carbon (C_{60}-FMC) with Bimodal Pores: XRD, TEM, Structural Properties, NMR, and Protein Immobilization. Int J Nanomater Nanotechnol Nanomed 2(1): 001-008. DOI: 10.17352/2455-3492.000006*

47. Militello V, Casarino C, Emanuele A, Giostra A, Pullara F, et al. (2004) Aggregation kinetics of bovine serum albumin studied by FTIR spectroscopy and light scattering. Biophysical Chemistry 107: 175-187.

48. Park M, Park SS, Selvaraj M, Kim I, Ha CS (2011) Hydrophobic periodic mesoporous organosilicas for the adsorption of cytochrome c. J Porous Mater 18: 217-223.

49. Zhou Z, Inayat A, Schwieger W, Hartman M (2012) Improved activity and stability of lipase immobilized in cage-like large pore mesoporous organosilicas. Micropor Mesopor Mater 154: 133-144.

50. Wahab MA, Darain F (2014) Nano-hard template synthesis of pure mesoporous NiO and its application for streptavidin protein immobilization. Nanotechnology 25: 165701.

51. Darain F, Chan WY, Chian HS (2011) Performance of surface-modified polycaprolactone on growth factor binding, release, and proliferation of smooth muscle Cells. Soft Mater 9: 64-78.

52. Darain F, Wahab MA, Tjin SW (2012) Surface Activation of Poly(Methyl methacrylate) by Plasma Treatment: Stable Antibody Immobilization for Microfluidic Enzyme-Linked Immunosorbent Assay. Analytical Lett 45: 25692579.

Citation: *Wahab MA, Darain F, Karim A, Beltramini JN (2016) Nano-Confined Synthesis of Fullerene Mesoporous Carbon (C_{60}-FMC) with Bimodal Pores: XRD, TEM, Structural Properties, NMR, and Protein Immobilization. Int J Nanomater Nanotechnol Nanomed 2(1): 001-008. DOI: 10.17352/2455-3492.000006*